Original Article
Pravastatin stimulates angiogenesis in a murine hindlimb ischemia model: a positron emission tomography imaging study with ^{64}Cu-NOTA-TRC105

Hakan Orbay[1], Hao Hong[1], Jill M Koch[2], Hector F Valdovinos[3], Timothy A Hacker[2], Charles P Theuer[4], Todd E Barnhart[3], Weibo Cai[1,3,5]

[1]Department of Radiology, University of Wisconsin - Madison, WI, USA; [2]Department of Medicine, University of Wisconsin - Madison, WI, USA; [3]Department of Medical Physics, University of Wisconsin - Madison, WI, USA; [4]TRACON Pharmaceuticals, Inc., San Diego, CA, USA; [5]University of Wisconsin Carbone Cancer Center, Madison, WI, USA

Abstract: In this study, ^{64}Cu-NOTA-TRC105 (TRC105 is an anti-CD105 monoclonal antibody that binds to both human and murine CD105) positron emission tomography (PET) was used to assess the response to pravastatin treatment in a murine model of peripheral artery disease (PAD). Hindlimb ischemia was induced by ligation of the right femoral arteries in BALB/c mice under anesthesia, and the left hindlimb served as an internal control. Mice in the treatment group were given intraperitoneal pravastatin daily until the end of the study, whereas the animals in the control group were injected with 0.9% sodium chloride solution. Laser Doppler imaging showed that blood flow in the ischemic hindlimb plummeted to ~20% of the normal level after surgery, and gradually recovered to near normal level on day 10 in the treatment group and on day 20 in the control group. Angiogenesis was non-invasively monitored and quantified with ^{64}Cu-NOTA-TRC105 PET on postoperative days 3, 10, 17, and 24. Tracer uptake at 48 h post-injection in the ischemic hindlimb in the treatment group was significantly higher than that of the control group on day 10 (20.5 ± 1.9 %ID/g vs 11.4 ± 1.5 %ID/g), suggesting increased CD105 expression and higher level of angiogenesis upon pravastatin treatment, and gradually decreased to background levels in both groups (4.9 ± 0.8 %ID/g vs 3.4 ± 1.9 %ID/g on day 24). The in vivo PET data correlated well with ex vivo biodistribution studies performed on day 24. Increased CD105 expression on days 3 and 10 following ischemia was further confirmed by immunofluorescence staining. Taken together, our results indicated that ^{64}Cu-NOTA-TRC105 PET is a suitable and non-invasive method to monitor the angiogenesis and therapeutic response in PAD, which can also be utilized for non-invasive evaluation of other pro-angiogenic/anti-angiogenic drugs in other cardiovascular diseases and cancer.

Keywords: Angiogenesis, ischemia, positron emission tomography (PET), peripheral artery disease (PAD), pravastatin, CD105 (endoglin)

Introduction

Peripheral artery disease (PAD) is a common manifestation of systemic atherosclerosis and its frequency is strongly related to age, rising steeply at older ages [1, 2]. Control of cardiovascular risk factors and stimulation of angiogenesis is mandatory in all patients to improve the prognosis of PAD. Conservative treatment can be effective, which is based on pharmacologic agents (e.g. cholesterol-lowering drugs), exercise therapy, etc, whereas surgical revascularization and endovascular interventions are usually restricted to symptomatic patients who do not respond to or tolerate medical therapy [2]. It has been shown that therapy with statin group of cholesterol-lowering drugs may improve walking distance and reduce the risk of developing new symptoms or worsening claudication in patients with PAD [3]. The mechanisms by which cholesterol-lowering drugs influence neovascularization in PAD could be attributed to the improvement of endothelial function, inhibition of inflammation, modulation of cardiovascular remodeling, among others.

Pravastatin, a member of statin group of cholesterol-lowering drugs, inhibits the enzyme

hydroxymethylglutaryl-CoA (HMG-CoA) reductase [4]. It has been used for the treatment of ischemic conditions in addition to hypercholesterolemia [4-7], because of its well-known pleiotropic effects [8]. For the follow-up of patients, reliable and non-invasive imaging methods that can assess the efficacy of pro-angiogenic treatment in PAD are needed [9, 10]. Various imaging techniques can detect changes in extremity blood circulation [10, 11]. However, only molecular imaging can provide information on both early molecular abnormalities that contribute to the development of PAD and the effects of the treatment on the ischemic tissues, thereby permitting early intervention and prompt adjustment of the treatment protocol.

Many molecular markers of angiogenesis, such as vascular endothelial growth factor receptor (VEGFR) and integrins, have been targeted for molecular imaging of angiogenesis [12]. Another emerging target that has gained increasing attention is CD105 (endoglin), a 180 kDa disulfide-linked homodimeric transmembrane protein that is selectively expressed on the endothelial cells of newly formed vessels [13]. We have recently developed a positron emission tomography (PET) tracer for non-invasive imaging of CD105 expression, ^{64}Cu-NOTA-TRC105 [14, 15], where TRC105 is a chimeric monoclonal antibody that binds to both human and murine CD105 and NOTA denotes 1,4,7-triazacyclononane-1,4,7-triacetic acid. The CD-105 specificity of ^{64}Cu-NOTA-TRC105 in vitro and in vivo has been extensively characterized in our previous reports though flow cytometry, microscopy, in vivo imaging, blocking, as well as ex vivo histological studies [14, 15]. In this work, we report the use of ^{64}Cu-NOTA-TRC105 PET for non-invasive and quantitative monitoring of pravastatin-induced angiogenesis in a murine hindlimb ischemia model of PAD.

Materials and methods

Synthesis and characterization of ^{64}Cu-NOTA-TRC105

TRC105 was provided by TRACON Pharmaceuticals (San Diego, CA) and S-2-(4-isothiocyanatobenzyl)-1,4,7-triazacyclononane-1,4,7-triacetic acid (p-SCN-Bn-NOTA) was purchased from Macrocyclics, Inc. (Dallas, TX). ^{64}Cu was produced with a CTI RDS 112 cyclotron using the ^{64}Ni(p,n)^{64}Cu reaction, which has a specific activity of > 5 Ci/μmol at the end-of-bombardment. Detailed synthesis and in vitro/in vivo characterization of ^{64}Cu-NOTA-TRC105 have been reported previously [14, 15]. In brief, NOTA conjugation was carried out at pH 9.0, with the ratio of p-SCN-Bn-NOTA:TRC105 being 25:1. NOTA-TRC105 was purified using PD-10 columns (GE Healthcare, Buckinghamshire, UK) with phosphate-buffered saline (PBS; HyClone laboratories, Logan, UT) as the mobile phase. For radiolabeling, ^{64}CuCl$_2$ (74 MBq) was diluted in 300 μL of 0.1 M sodium acetate buffer (pH 5.5) and added to 50 μg of NOTA-TRC105. The reaction mixture was incubated for 30 min at 37 °C with constant shaking. ^{64}Cu-NOTA-TRC105 was purified using PD-10 columns with PBS as the mobile phase. The radioactive fractions containing ^{64}Cu-NOTA-TRC105 were collected and passed through a 0.2 μm syringe filter for in vivo experiments.

Induction of hindlimb ischemia in mice

All animal studies were conducted under a protocol approved by the University of Wisconsin Institutional Animal Care and Use Committee. Right unilateral hindlimb ischemia was induced in six-week-old female BALB/c mice (Harlan, Indianapolis, IN). Animals were anesthetized with 2% isoflurane. The femoral triangle was exposed by a modified oblique incision at mid-abdominal level. Right femoral artery was separated from femoral vein and nerve by blunt dissection distal to the inguinal ligament. The artery was tied proximally and distally with a 7/0 nylon suture (AROSurgical Corp., Newport Beach, CA) and cut sharply between the two sutures. A sham procedure was performed on the contralateral hindlimb to serve as the internal control. Of note, the reason for placing the incision at the mid-abdominal level was to eliminate the possibility of superposition of radioactivity signals from surgical wound and the ischemic muscle tissue.

Pravastatin treatment

After the operation, mice were randomly divided into 2 groups (7 mice in the treatment group and 6 mice in the control group). Pravastatin, dissolved in 0.9% sodium chloride solution (Hospira Inc., Lake Forest, IL), was injected intraperitoneally (i.p.) into the mice in the treatment group at a dose of 2 mg/kg every day starting from postoperative day 1 until the end of study (postoperative day 24). The dose of

pravastatin was determined according to previous studies [4]. Mice in the control group received i.p. injection of 0.9% sodium chloride solution daily.

Laser Doppler imaging of hindlimb perfusion

Three mice from each group were used for serial laser Doppler imaging studies. Baseline laser Doppler images were obtained before surgery and soon after surgery with a laser Doppler imaging system (moorLDI2-HR, Moor instruments, DE, USA). Subsequently, the recovery of the ischemic hindlimb was followed by serial images obtained on postoperative days 3, 10, 13, 17, 20, and 24. The mice were kept at 37 °C throughout the procedure. Average blood perfusion in both hindlimb was measured using region-of-interest (ROI) analysis. The results were expressed as the ratio of ischemic to non-ischemic hindlimb perfusion.

PET imaging and biodistribution studies

Four mice from the pravastatin treatment group and 3 mice from the control group were subjected to serial PET imaging studies on an Inveon microPET/microCT rodent model scanner (Siemens Medical Solutions USA, Inc.). Data acquisition, image reconstruction, and ROI analysis were carried out in a similar fashion as our previous reports [16-19]. Each mouse was intravenously injected with 5-10 MBq of ^{64}Cu-NOTA-TRC105 and five- to ten-minute static PET scans were performed at various time points post-injection (p.i.) with the animals maintained under 2% isoflurane anesthesia. Quantitative PET data were presented as percentage injected dose per gram of tissue (%ID/g).

Immediately after the PET scans on postoperative day 24, biodistribution studies were carried out to confirm that the quantitative tracer uptake values based on PET imaging and ROI analysis accurately represented the radioactivity distribution. Blood, hindlimb muscle tissue, and major organs and tissues were harvested and wet-weighted. The radioactivity in the tissue was measured using a Cobra II γ-counter (Perkin-Elmer) and presented as %ID/g.

Histology

Muscle tissues from both the ischemic and control hindlimb were frozen in Tissue-Tek O.C.T compound (Sakura Finetek U.S.A., Inc. CA).

Frozen tissue blocks were cut into 5 µm thick slices and fixed with cold acetone for 10 min. Following blocking with 10% donkey serum for 30 min at room temperature, the slices were incubated with a mixture of TRC105 (5 µg/mL) and rat anti-mouse CD31 antibody (BD biosciences, San Jose, CA) for 1 h at room temperature. Positive areas were visualized using AlexaFluor488-labeled goat anti-human IgG (Invitrogen, Eugene, OR) and Cy3-labeled donkey anti-rat IgG (Jackson laboratories, West Grove, PA) respectively as the secondary antibodies. All images were acquired with a Nikon Eclipse Ti microscope.

Statistical analysis

Data were presented as mean ± SD. The data from different groups were compared with 1-way ANOVA followed by the Tukey's post hoc test if necessary. Differences were considered as statistically significant when $P < 0.05$. Data were analyzed with IBM SPSS Statistics 16.0.

Results

^{64}Cu-labeling of TRC105

^{64}Cu-labeling including final purification using size exclusion column chromatography took 80 ± 10 min (n = 5). The decay-corrected radiochemical yield was > 85% based on 25 µg of NOTA-TRC105 per 37 MBq of ^{64}Cu, and the radiochemical purity was > 98%. The specific activity of ^{64}Cu-NOTA-TRC105 was about 1.2 GBq/mg of protein, assuming complete recovery of NOTA-TRC105 after size exclusion column chromatography.

Laser Doppler imaging of hindlimb perfusion

Laser Doppler imaging was performed to confirm the successful induction of tissue ischemia following femoral artery ligation (**Figure 1A**). Soon after ligation, the average hindlimb tissue perfusion ratio decreased from 0.90 ± 0.10 to 0.22 ± 0.08 (n = 3) in the control group and from 1.06 ± 0.28 to 0.19 ± 0.04 (n = 3) in the pravastatin treatment group. Over the next several weeks, hindlimb tissue perfusion ratio in the control group on days 3, 10, 13, 17, 20, and 24 was 0.35 ± 0.13, 0.58 ± 0.22, 0.58 ± 0.05, 0.81 ± 0.24, 0.89 ± 0.43, and 0.91 ± 0.24 respectively (n = 3; **Figure 1B**). Hindlimb tissue perfusion ratio in mice treated with pravastatin on days 3, 10, 13, 17, 20, and 24 was 0.46 ±
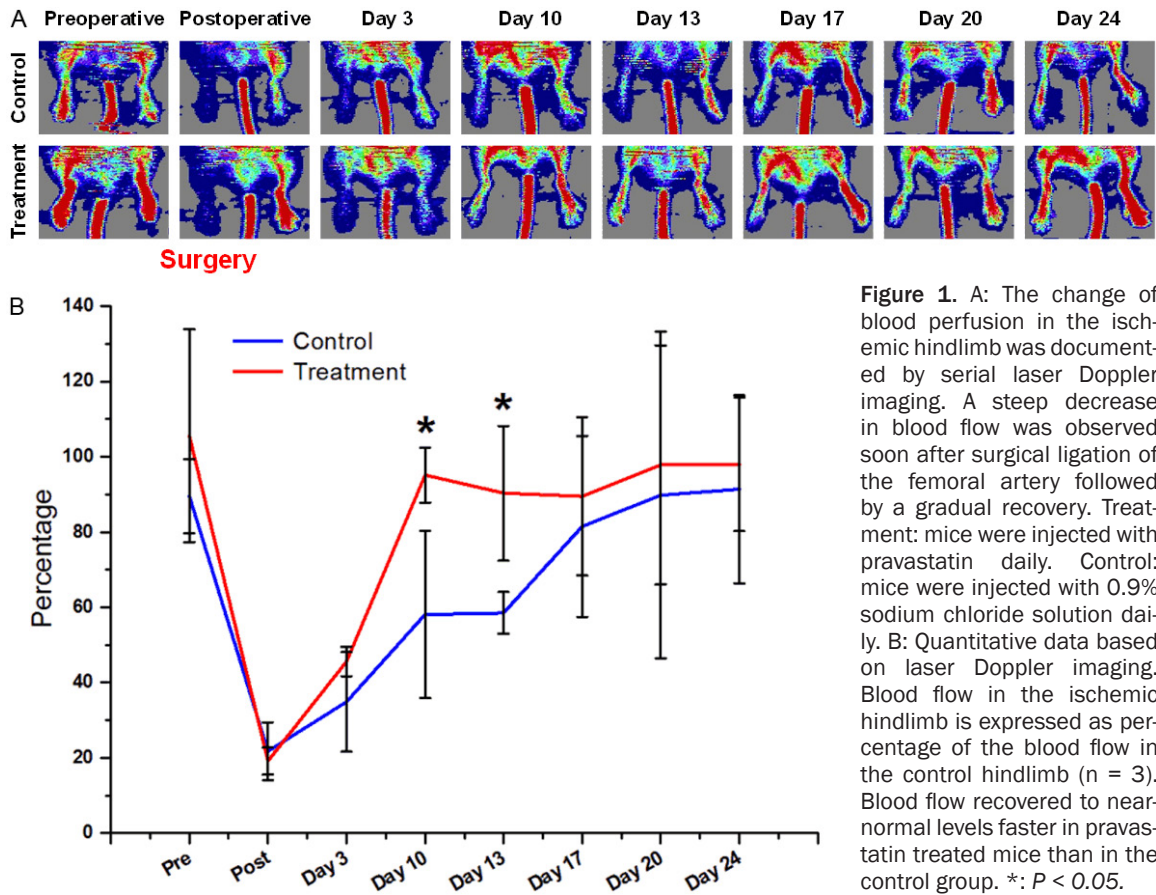
Figure 1. A: The change of blood perfusion in the ischemic hindlimb was documented by serial laser Doppler imaging. A steep decrease in blood flow was observed soon after surgical ligation of the femoral artery followed by a gradual recovery. Treatment: mice were injected with pravastatin daily. Control: mice were injected with 0.9% sodium chloride solution daily. B: Quantitative data based on laser Doppler imaging. Blood flow in the ischemic hindlimb is expressed as percentage of the blood flow in the control hindlimb (n = 3). Blood flow recovered to near-normal levels faster in pravastatin treated mice than in the control group. *: P < 0.05.

0.04, 0.95 ± 0.07, 0.90 ± 0.18, 0.89 ± 0.21, 0.98 ± 0.32, and 0.98 ± 0.18 respectively. The differences between the two groups were statistically significant on days 10 and 13 (*P < 0.05*). Overall, the perfusion in ischemic hindlimb recovered to normal level as early as day 10 in mice treated with pravastatin, whereas perfusion in the ischemic hindlimb did not return to normal levels until day 20 in the control group, suggesting that pravastatin can stimulate angiogenesis after surgical induction of hindlimb ischemia.

PET imaging and biodistribution studies

64Cu-NOTA-TRC105 PET was carried out on days 3, 10, 17, and 24 after surgery to monitor CD105 expression non-invasively (**Figure 2A**). On the basis of our previous experience with in vivo PET imaging of angiogenesis using TRC105-based agents [14, 15, 20], the time points of 4, 24, and 48 h p.i. were chosen for serial PET scans. At 4 h p.i., there was a relatively high level of blood radioactivity and background signal because of the long circulation

half-life of the radiolabeled antibody. 64Cu-NOTA-TRC105 uptake in the tissue of interest (e.g. tumor and ischemic tissue) typically plateaued between 24 and 48 h p.i. [14, 15, 20]. Of note, since we placed the initial incision in the mid-abdominal level, which is well separated from the ischemic hindlimb, there was no superposition of PET signals from the ischemic muscle and the scar tissue (high level of angiogenesis is also observed during wound healing).

Uptake of 64Cu-NOTA-TRC105 in the ischemic hindlimb was the highest at 48 h p.i., at 14.1 ± 1.6, 11.4 ± 1.5, 6.2 ± 1.5, and 3.4 ± 1.9 %ID/g for the control group on days 3, 10, 17, and 24 after surgery, respectively (n = 3; **Figure 2B**). 64Cu-NOTA-TRC105 uptake in the ischemic hindlimb at 48 h p.i. in the pravastatin treated mice were 16.4 ± 0.8, 20.5 ± 1.9, 6.9 ± 0.9, and 4.9 ± 0.8 %ID/g on days 3, 10, 17, and 24 after surgery, respectively (n = 4). Comparing the two groups, tracer uptake was significantly different on day 10 after surgery, corroborating the laser Doppler imaging results where pravastatin treated mice have higher level of ischemic
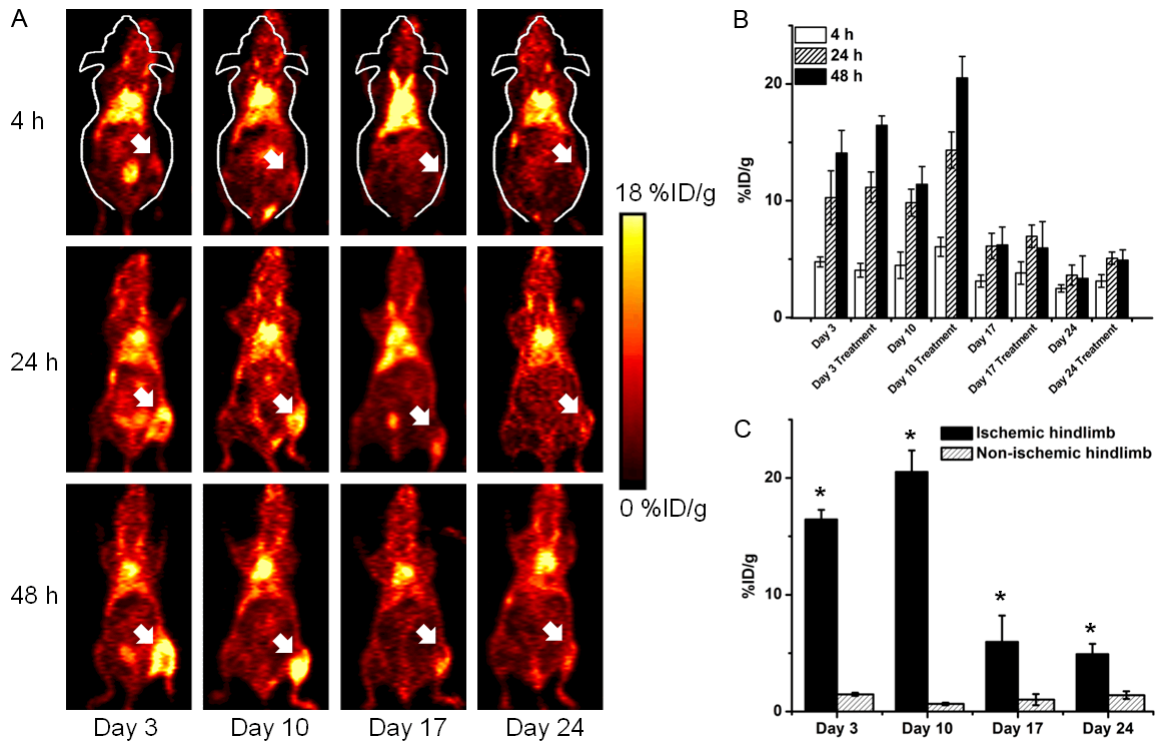
Figure 2. A: Representative coronal PET images at 4, 24, and 48 h post-injection of ^{64}Cu-NOTA-TRC105 on days 3, 10, 17, and 24 after surgical induction of hindlimb ischemia (white arrows) and daily pravastatin treatment. B: %ID/g values of ^{64}Cu-NOTA-TRC105 uptake in the ischemic hindlimb at 4, 24, and 48 h post-injection on days 3, 10, 17, and 24 after surgery, with (n = 4) or without (n = 3) daily pravastatin treatment. C: In the pravastatin treated mice, the differences between ^{64}Cu-NOTA-TRC105 uptake in the ischemic and non-ischemic hindlimb were statistically significant at all time points examined. n = 4. *: *P < 0.05.*

hindlimb perfusion and angiogenesis than mice treated with saline. ^{64}Cu-NOTA-TRC105 uptake in the non-operated hindlimb were comparable in the two groups (1.9 ± 0.2, 1.5 ± 0.5, 1.5 ± 0.3, and 1.9 ± 0.3 %ID/g for the control group [n = 3] and 1.5 ± 0.1, 0.6 ± 0.1, 1.2 ± 0.1, and 1.4 ± 0.3 for the treatment group [n = 4] on days 3, 10, 17, and 24 respectively), significantly lower than that in the ischemic hindlimb in all cases (**Figure 2C**). Ex vivo biodistribution data of ^{64}Cu-NOTA-TRC105 in blood, major organs, and tissues after the last PET scans at 48 h p.i. are summarized in **Figure 3**, which corroborated the findings from non-invasive PET scans and confirmed that PET imaging enabled accurate quantification of ^{64}Cu-NOTA-TRC105 uptake in mice.

Histology

Representative CD31/CD105 co-staining images of the ischemic hindlimb muscle in the pravastatin treated group are shown in **Figure 4**. The highest density of CD105 positive ves-

sels was observed on postoperative day 3 (393 ± 72 vessels/mm^2; n = 5) and day 10 (502 ± 54 vessels/mm^2; n = 5). The average number of CD105 positive vessels dropped to 84 ± 30 vessels/mm^2 (n = 5) on day 17, whereas no significant CD105 staining was observed on day 24. The difference in CD105 positive vessel density between postoperative days 3 and 10 was not statistically significant, while the difference between day 17 and day 10 (or day 3) was statistically significant (P < 0.05). On day 10, the CD105 positive vessel density in the pravastatin treated group was significantly higher than that of the control group (279 ± 191 vessels/mm^2; n = 5), further validating the in vivo laser Doppler and PET imaging results and confirmed that pravastatin could stimulate angiogenesis in the ischemic hindlimb.

Discussion

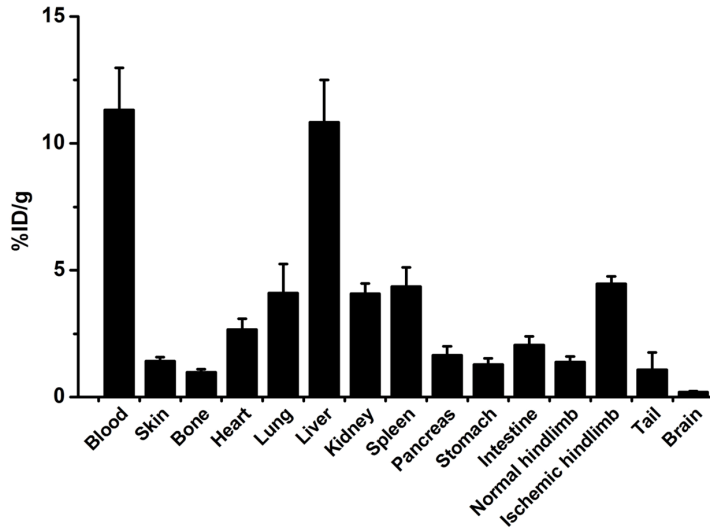In a previous study, we have demonstrated that ^{64}Cu-NOTA-TRC105 PET is a suitable technique

Figure 3. Biodistribution of ^{64}Cu-NOTA-TRC105 in major organs at 48 h post-injection on postoperative day 24 in pravastatin treated mice.

for non-invasive imaging of ischemia-induced angiogenesis in a murine model of PAD [14], where a variety of in vitro, in vivo, and ex vivo experiments were performed to thoroughly characterize the tracer and confirm its CD105 specificity in vivo. In this work, we demonstrated that PET is also a suitable technique to monitor the therapeutic response in this model, where non-invasive PET imaging could easily detect increased uptake of ^{64}Cu-NOTA-TRC105 (representing CD105 expression level and angiogenesis) in response to pravastatin treatment. The temporal course of tracer uptake was slightly different from the previous study (which peaked at day 3 after surgery), reaching a peak on day 10 following surgery and daily pravastatin treatment, which correlated well with CD105 expression levels as documented by immunofluorescence staining. This phenomenon is likely due to the existence of a latent period for pravastatin to elicit its pro-angiogenic effects and the time it takes for new blood vessels to sprout and grow in the ischemic hindlimb.

Various studies have indicated that the statin group drugs can restore ischemic limb blood flow via upregulation of eNOS/NO (eNOS: endothelial nitric oxide synthase; NO: nitric oxide) [21]. Statins can activate protein kinase B (also known as Akt) and facilitate the Akt-eNOS interaction in endothelial cells, thereby promoting the activation/phosphorylation of eNOS and

NO-mediated angiogenesis [22, 23]. In other reports, it has been suggested that statins can enhance the stability of eNOS mRNA [24]. Another possible mechanism of action for statins is the mobilization of endothelial progenitor cells from bone marrow, which can facilitate their incorporation into the neovasculature of ischemic tissues [25].

A reliable, non-invasive imaging method to monitor the molecular changes during the course of ischemic diseases has long been sought after. Molecular imaging methods including PET have significant advantages over conventional vascular imaging techniques such as contrast angiography, magnetic resonance (MR) angiography, and computed tomography (CT) angiography [26]. Contrast angiography provides detailed information on the vascular anatomy and blood circulation in the ischemic tissue, but it is an invasive technique that requires significant skills and expertise. Newer generation vascular imaging strategies (e.g. high resolution MR/CT angiography) are less invasive than the conventional techniques, however they cannot detect changes at the molecular level hence are not ideal for (guiding) early intervention. PET imaging with small molecules (e.g. ^{13}N-NH$_3$, ^{15}O-H$_2$O, and ^{11}C-CO$_2$) to measure extremity blood flow is similar as conventional angiography, which does not provide sufficient information on the molecular mechanisms of tissue ischemia and treatment response [27-29].

Laser Doppler perfusion imaging is frequently used to examine hindlimb perfusion and it can give relatively consistent results in small animal models. The major limitation of this technique is the limited imaging depth, which cannot provide reliable information on the subtle changes in blood flow in deeper tissues. In addition, laser Doppler imaging is mainly used for relative blood flow measurements rather than accurate absolute measurement of blood flow [30]. Furthermore, inflammation resulting from skin trauma and release of inflammatory paracrine factors (e.g. histamine) may lead to significant alterations in blood flow measure-
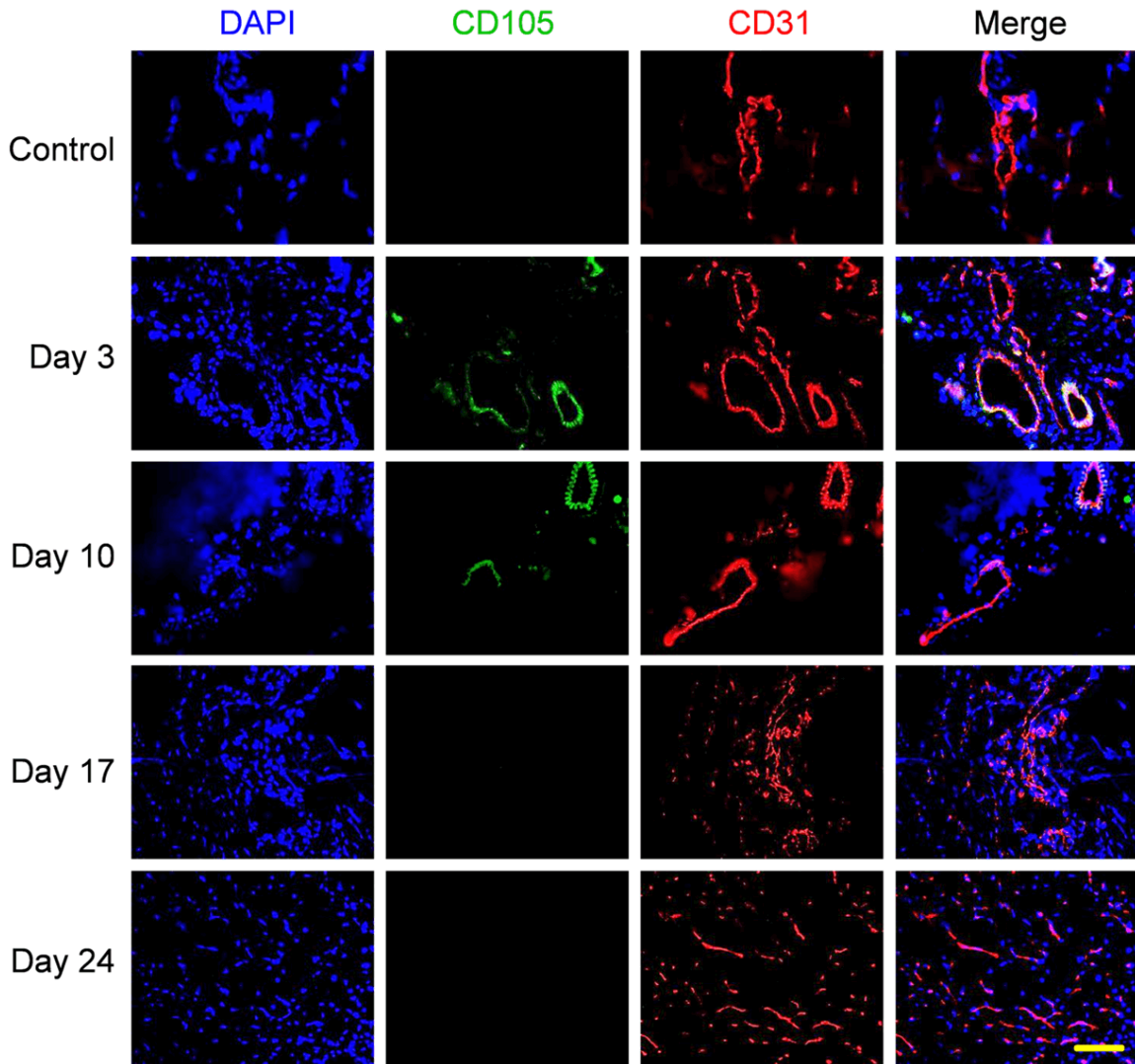
Figure 4. Immunofluorescence staining showed increased CD105 expression in the ischemic hindlimb on postoperative days 3 and 10 after daily pravastatin treatment, significantly higher than that on days 17 and 24, as well as the control non-ischemic hindlimb. Green: CD105; red: CD31; blue: DAPI. Scale bar: 100 μm.

ment with laser Doppler [31]. In this study, the results of laser Doppler imaging and PET imaging correlated quite well, due to the superficial location of blood vessels in the mouse hindlimb. However, discrepancy between PET and laser Doppler imaging results is anticipated in the cases of larger animal models and human studies.

PET imaging can offer invaluable biological insights on the mechanisms underlying ischemia and the response of ischemia to treatment, as demonstrated in this work. Previous literature reports on PET imaging of PAD have addressed the potential roles of different radionuclides (e.g., ^{64}Cu, ^{68}Ga, and ^{76}Br) and tracers

for visualization and quantification of various molecular markers of angiogenesis under ischemic conditions [32-34]. ^{64}Cu was used as the PET isotope in this study due to its wide availability, low cost, and versatile chemistry [35, 36]. The E_{max} of ^{64}Cu (656 keV) for its positron emission is comparable to ^{18}F, which can give PET images with good quality and spatial resolution.

VEGF/VEGFR and $\alpha_v\beta_3$ integrin are some of the most commonly targeted markers of angiogenesis for imaging applications [12, 37-40]. CD105 is expressed at much higher levels than VEGFR and $\alpha_v\beta_3$ integrin on actively proliferating endothelial cells, which make it highly desir-

able for imaging applications [41]. Tracer uptake in the ischemic hindlimb was typically reported to be < 2 %ID/g in previous literature reports using other tracers [28, 32-34], whereas uptake of ^{64}Cu-NOTA-TRC105 in this study was 10-fold higher (~20 %ID/g). It is worth noting that the signaling pathways of VEGF/VEGFR and CD105 are distinct [42]. Therefore, PET imaging with tracers that are specific for each of these pathways is expected to provide complementary information in future studies.

Conclusion

^{64}Cu-NOTA-TRC105 PET is a suitable non-invasive tool to monitor the changes in angiogenesis level and CD105 expression in response to pravastatin treatment in a murine model of PAD. Tracer uptake in the ischemic hindlimb was persistent and corresponds to the changes in CD105 expression level, as validated by various in vivo and ex vivo experiments, which can be translated into the clinic for non-invasive evaluation of angiogenesis. Not limited to PAD, ^{64}Cu-NOTA-TRC105 PET can also be utilized for non-invasive evaluation of other pro-angiogenic/anti-angiogenic drugs in other cardiovascular diseases and cancer.

Acknowledgements

Disclosure of conflict of interest

CPT is an employee of TRACON Pharmaceuticals, Inc. The other authors declare no conflict of interest.

Address correspondence to: Dr. Weibo Cai, Departments of Radiology and Medical Physics, School of Medicine and Public Health, University of Wisconsin - Madison, Room 7137, 1111 Highland Ave, Madison, WI 53705-2275, USA. Tel: 1-608-262-1749; Fax: 1-608-265-0614; E-mail: wcai@uwhealth.org

References

[1] Sumner AD, Khalil YK and Reed JF 3rd. The relationship of peripheral arterial disease and metabolic syndrome prevalence in asymptomatic US adults 40 years and older: results from the National Health and Nutrition Examination Survey (1999-2004). J Clin Hypertens (Greenwich) 2012; 14: 144-148.

[2] Simmons A, Steffen K and Sanders S. Medical therapy for peripheral arterial disease. Curr Opin Cardiol 2012; 27: 592-597.

[3] Gargiulo G, Giugliano G, Brevetti L, Sannino A, Schiattarella GG, Serino F, Carbone A, Scudiero F, Ferrone M, Corrado R, Izzo R, Chiariotti L, Perrino C, Amato B, Trimarco B and Esposito G. Use of statins in lower extremity artery disease: a review. BMC Surg 2012; 12 Suppl 1: S15.

[4] Berger C, Xia F, Maurer MH and Schwab S. Neuroprotection by pravastatin in acute ischemic stroke in rats. Brain Res Rev 2008; 58: 48-56.

[5] Haslinger-Loffler B. Multiple effects of HMG-CoA reductase inhibitors (statins) besides their lipid-lowering function. Kidney Int 2008; 74: 553-555.

[6] Mariucci G, Taha E, Tantucci M, Spaccatini C, Tozzi A and Ambrosini MV. Intravenous administration of pravastatin immediately after middle cerebral artery occlusion reduces cerebral oedema in spontaneously hypertensive rats. Eur J Pharmacol 2011; 660: 381-386.

[7] Abe Y, Izumi T, Urabe A, Nagai M, Taniguchi I, Ikewaki K and Mochizuki S. Pravastatin prevents myocardium from ischemia-induced fibrosis by protecting vascular endothelial cells exposed to oxidative stress. Cardiovasc Drugs Ther 2006; 20: 273-280.

[8] Davignon J. Beneficial cardiovascular pleiotropic effects of statins. Circulation 2004; 109: III39-43.

[9] van Weel V, van Tongeren RB, van Hinsbergh VW, van Bockel JH and Quax PH. Vascular growth in ischemic limbs: a review of mechanisms and possible therapeutic stimulation. Ann Vasc Surg 2008; 22: 582-597.

[10] Orbay H, Hong H, Zhang Y and Cai W. PET/SPECT imaging of hindlimb ischemia: focusing on angiogenesis and blood flow. Angiogenesis 2013; 16: 279-287.

[11] Cavalcanti Filho JL, de Souza Leao Lima R, de Souza Machado Neto L, Kayat Bittencourt L, Domingues RC and da Fonseca LM. PET/CT and vascular disease: current concepts. Eur J Radiol 2011; 80: 60-67.

[12] Cai W and Chen X. Multimodality molecular imaging of tumor angiogenesis. J Nucl Med 2008; 49 Suppl 2: 113S-128S.

[13] Fonsatti E, Nicolay HJ, Altomonte M, Covre A and Maio M. Targeting cancer vasculature via endoglin/CD105: a novel antibody-based diag-

nostic and therapeutic strategy in solid tumours. Cardiovasc Res 2010; 86: 12-19.

[14] Orbay H, Zhang Y, Hong H, Hacker TA, Valdovinos HF, Zagzebski JA, Theuer CP, Barnhart TE and Cai W. Positron Emission Tomography Imaging of Angiogenesis in a Murine Hindlimb Ischemia Model with Cu-Labeled TRC105. Mol Pharm 2013; 10: 2749-2756.

[15] Zhang Y, Hong H, Engle JW, Bean J, Yang Y, Leigh BR, Barnhart TE and Cai W. Positron emission tomography imaging of CD105 expression with a ^{64}Cu-labeled monoclonal antibody: NOTA is superior to DOTA. PLoS One 2011; 6: e28005.

[16] Xiao Y, Hong H, Matson VZ, Javadi A, Xu W, Yang Y, Zhang Y, Engle JW, Nickles RJ, Cai W, Steeber DA and Gong S. Gold Nanorods Conjugated with Doxorubicin and cRGD for Combined Anticancer Drug Delivery and PET Imaging. Theranostics 2012; 2: 757-768.

[17] Zhang Y, Hong H, Engle JW, Yang Y, Barnhart TE and Cai W. Positron Emission Tomography and Near-Infrared Fluorescence Imaging of Vascular Endothelial Growth Factor with Dual-Labeled Bevacizumab. Am J Nucl Med Mol Imaging 2012; 2: 1-13.

[18] Zhang Y, Hong H, Severin GW, Engle JW, Yang Y, Goel S, Nathanson AJ, Liu G, Nickles RJ, Leigh BR, Barnhart TE and Cai W. ImmunoPET and near-infrared fluorescence imaging of CD105 expression using a monoclonal antibody dual-labeled with [89]Zr and IRDye 800CW. Am J Transl Res 2012; 4: 333-346.

[19] Hong H, Benink HA, Uyeda HT, Valdovinos HF, Zhang Y, Meisenheimer P, Barnhart TE, Fan F and Cai W. HaloTag as a reporter gene: positron emission tomography imaging with ^{64}Cu-labeled second generation HaloTag ligands. Am J Transl Res 2013; 5: 291-302.

[20] Hong H, Yang Y, Zhang Y, Engle JW, Barnhart TE, Nickles RJ, Leigh BR and Cai W. Positron emission tomography imaging of CD105 expression during tumor angiogenesis. Eur J Nucl Med Mol Imaging 2011; 38: 1335-1343.

[21] Fujii T, Onimaru M, Yonemitsu Y, Kuwano H and Sueishi K. Statins restore ischemic limb blood flow in diabetic microangiopathy via eNOS/NO upregulation but not via PDGF-BB expression. Am J Physiol Heart Circ Physiol 2008; 294: H2785-2791.

[22] Dimmeler S, Fleming I, Fisslthaler B, Hermann C, Busse R and Zeiher AM. Activation of nitric oxide synthase in endothelial cells by Akt-dependent phosphorylation. Nature 1999; 399: 601-605.

[23] Fulton D, Gratton JP, McCabe TJ, Fontana J, Fujio Y, Walsh K, Franke TF, Papapetropoulos A and Sessa WC. Regulation of endothelium-de-

rived nitric oxide production by the protein kinase Akt. Nature 1999; 399: 597-601.

[24] Laufs U and Liao JK. Post-transcriptional regulation of endothelial nitric oxide synthase mRNA stability by Rho GTPase. J Biol Chem 1998; 273: 24266-24271.

[25] Dimmeler S, Aicher A, Vasa M, Mildner-Rihm C, Adler K, Tiemann M, Rutten H, Fichtlscherer S, Martin H and Zeiher AM. HMG-CoA reductase inhibitors (statins) increase endothelial progenitor cells via the PI 3-kinase/Akt pathway. J Clin Invest 2001; 108: 391-397.

[26] Dobrucki LW and Sinusas AJ. PET and SPECT in cardiovascular molecular imaging. Nat Rev Cardiol 2010; 7: 38-47.

[27] Penuelas I, Aranguren XL, Abizanda G, Marti-Climent JM, Uriz M, Ecay M, Collantes M, Quincoces G, Richter JA and Prosper F. ^{13}N-ammonia PET as a measurement of hindlimb perfusion in a mouse model of peripheral artery occlusive disease. J Nucl Med 2007; 48: 1216-1223.

[28] Liu Y, Pressly ED, Abendschein DR, Hawker CJ, Woodard GE, Woodard PK and Welch MJ. Targeting angiogenesis using a C-type atrial natriuretic factor-conjugated nanoprobe and PET. J Nucl Med 2011; 52: 1956-1963.

[29] Depairon M, De Landsheere C, Merlo P, Del Fiore G, Quaglia L, Peters JM, Lamotte D and Zicot M. Effect of exercise on the leg distribution of C15O2 and 15O2 in normals and in patients with peripheral ischemia: a study using positron tomography. Int Angiol 1988; 7: 254-257.

[30] Briers JD. Laser Doppler, speckle and related techniques for blood perfusion mapping and imaging. Physiol Meas 2001; 22: R35-66.

[31] Clough G. Experimental models of skin inflammation. Clin Exp Allergy 1999; 29 Suppl 3: 105-108.

[32] Almutairi A, Rossin R, Shokeen M, Hagooly A, Ananth A, Capoccia B, Guillaudeu S, Abendschein D, Anderson CJ, Welch MJ and Frechet JM. Biodegradable dendritic positron-emitting nanoprobes for the noninvasive imaging of angiogenesis. Proc Natl Acad Sci U S A 2009; 106: 685-690.

[33] Jeong JM, Hong MK, Chang YS, Lee YS, Kim YJ, Cheon GJ, Lee DS, Chung JK and Lee MC. Preparation of a promising angiogenesis PET imaging agent: ^{68}Ga-labeled c(RGDyK)-isothiocyanatobenzyl-1,4,7-triazacyclononane-1,4,7-triacetic acid and feasibility studies in mice. J Nucl Med 2008; 49: 830-836.

[34] Willmann JK, Chen K, Wang H, Paulmurugan R, Rollins M, Cai W, Wang DS, Chen IY, Gheysens O, Rodriguez-Porcel M, Chen X and Gambhir SS. Monitoring of the biological response to murine hindlimb ischemia with ^{64}Cu-labeled

vascular endothelial growth factor-121 positron emission tomography. Circulation 2008; 117: 915-922.

[35] Wadas TJ, Wong EH, Weisman GR and Anderson CJ. Coordinating radiometals of copper, gallium, indium, yttrium, and zirconium for PET and SPECT imaging of disease. Chem Rev 2010; 110: 2858-2902.

[36] Wong AW, Ormsby E, Zhang H, Seo JW, Mahakian LM, Caskey CF and Ferrara KW. A comparison of image contrast with ^{64}Cu-labeled long circulating liposomes and ^{18}F-FDG in a murine model of mammary carcinoma. Am J Nucl Med Mol Imaging 2013; 3: 32-43.

[37] Cai W, Rao J, Gambhir SS and Chen X. How molecular imaging is speeding up antiangiogenic drug development. Mol Cancer Ther 2006; 5: 2624-2633.

[38] Alauddin MM. Positron emission tomography (PET) imaging with ^{18}F-based radiotracers. Am J Nucl Med Mol Imaging 2012; 2: 55-76.

[39] Chen F, Zhang Y and Cai W. Molecular MRI of VEGFR-2 reveals intra-tumor and inter-tumor heterogeneity. Am J Nucl Med Mol Imaging 2013; 3: 312-316.

[40] Liu S, Park R, Conti PS and Li Z. "Kit like" ^{18}F labeling method for synthesis of RGD peptide-based PET probes. Am J Nucl Med Mol Imaging 2013; 3: 97-101.

[41] Takahashi N, Haba A, Matsuno F and Seon BK. Antiangiogenic therapy of established tumors in human skin/severe combined immunodeficiency mouse chimeras by anti-endoglin (CD105) monoclonal antibodies, and synergy between anti-endoglin antibody and cyclophosphamide. Cancer Res 2001; 61: 7846-7854.

[42] Dallas NA, Samuel S, Xia L, Fan F, Gray MJ, Lim SJ and Ellis LM. Endoglin (CD105): a marker of tumor vasculature and potential target for therapy. Clin Cancer Res 2008; 14: 1931-1937.